npj | heritage science

Article

https://doi.org/10.1038/s40494-025-01712-z

The deterioration structure of tremolite jade artifacts from the Sanxingdui sacrificial pits dated to the Shang Dynasty in Guanghan, Sichuan, China

Check for updates

Chujing Xu[1,2], Jiancheng Liu[3], Yunpeng Wang[2,4] ✉, Honglin Ran[3], Haoze Wu[1,2], Hui Fang[1,2] & Qinglin Ma[5] ✉

The Sanxingdui archaeological site, located in Guanghan City, Sichuan Province, is considered one of the most significant archaeological discoveries in China. Current research suggests that jade artifacts unearthed from the sacrificial pits at the site were subjected to high temperatures before being interred, which led to the transformation of tremolite into whitened pyroxene. In this study, tremolite and pyroxene samples from the sacrificial pits at the Sanxingdui site were selected for analysis. These samples were examined using a variety of analytical techniques, including ultra-depth-of-field microscopy, scanning electron microscopy with X-ray energy dispersive spectrometry, laser confocal Raman spectroscopy, and Fourier transform infrared spectroscopy. The objective of this study was to investigate the structural characteristics and deterioration status of the jade artifacts. The results indicate that jade artifacts with a higher degree of pyroxenization tend to exhibit more severe deterioration, while tremolite jade artifacts without pyroxenization generally remain in better condition.

In 2020, the Sichuan Provincial Institute of Cultural Relics and Archaeology, in cooperation with other institutions, conducted a comprehensive excavation of sacrificial pits K3 to K8 at the Late Shang Dynasty site of the Sanxingdui (三星堆) (ca. 1200–1000 BC). This excavation unearthed numerous valuable relics, including bronze, gold, jade, and ivory[1–3]. A wide variety of jade artifacts were uncovered, including *zhang* (璋), *ge* (戈), *Zao* (凿), *yuan* (瑗), *jin* (斤), *Cong* (琮)[4]. Some jade artifacts had transformed into a white powdery state and lost their original shape.

Lu's research revealed evidence of a mineral thermal phase transition from tremolite to diopside in the jade artifacts from the K3–K8 sacrificial pits, thereby substantiating the occurrence of jade burning during sacrificial activities at the Sanxingdui site[5]. Guo's analyses of the chromaticity and magnetic properties within the pits support the hypothesis that these pits were used for the burial of burnt sacrificial offerings[6]. The phenomenon of jade burning can be traced back to the late Neolithic period in China. Scientific analyses indicate that jade burning occurred at various sites across different periods, such as the Liangzhu Sidun (良渚寺墩) site[7] and the Yinxu Fuhao tomb (殷墟妇好墓) of the Shang Dynasty[8], where burnt jade artifacts have been discovered.

The presence of notable whitening features in burnt jade artifacts has been a consistent subject of study in ancient jade research. This phenomenon has prompted scholars to propose various explanations[9]. Wang's research on the Raman spectra of whitened jade artifacts from the K3-K8 sacrificial pits revealed a characteristic hump-shaped fluorescence signal. In an oxygen-deficient environment, the crystal-enclosed organic matter within the jade undergone a high-temperature polymerization reaction in which the carbonyl groups are conjugated, resulting in fluorescence. The crystal-enclosed organic matter is derived from the magnesian carbonate, the parent rock of jade, and is mainly composed of waxes or resins and their corresponding ammonium or magnesium salts. In the imitation experiment, the jade rock was heated to 700 °C, thereby removing the adsorbed organic matter it contained. The jade rock was then immersed in a hydrochloric acid solution to facilitate its decomposition. Finally, the crystal-enclosed organic matter can be extracted using an organic solvent[10].

At present, most research on Sanxingdui jade artifacts has focused on mineral identification[4], chemical composition[11], and origin traceability[12], with comparatively few studies addressing the jade structure and

[1]Institute of Cultural Heritage, Shandong University, Qingdao, China. [2]Joint International Research Laboratory for Environmental and Social Archaeology of Shandong University, Qingdao, China. [3]Sichuan Provincial Institute of Cultural Relics and Archeology, Chengdu, China. [4]Shandong Provincial Cultural Relics Conservation, Restoration and Identification Center, Jinan, China. [5]Key Scientific Research Base of Science & Technology Evaluation, National Cultural Heritage Administration (Beijing University of Chemical Technology), Beijing, China. ✉e-mail: 215867190@qq.com; qinglinma226@126.com

Fig. 1 | Photographs of jade artifacts from the Sanxingdui (**a** K7QW-Y-32; **b** K7QW-Y-112; and **c** K3QW-557).

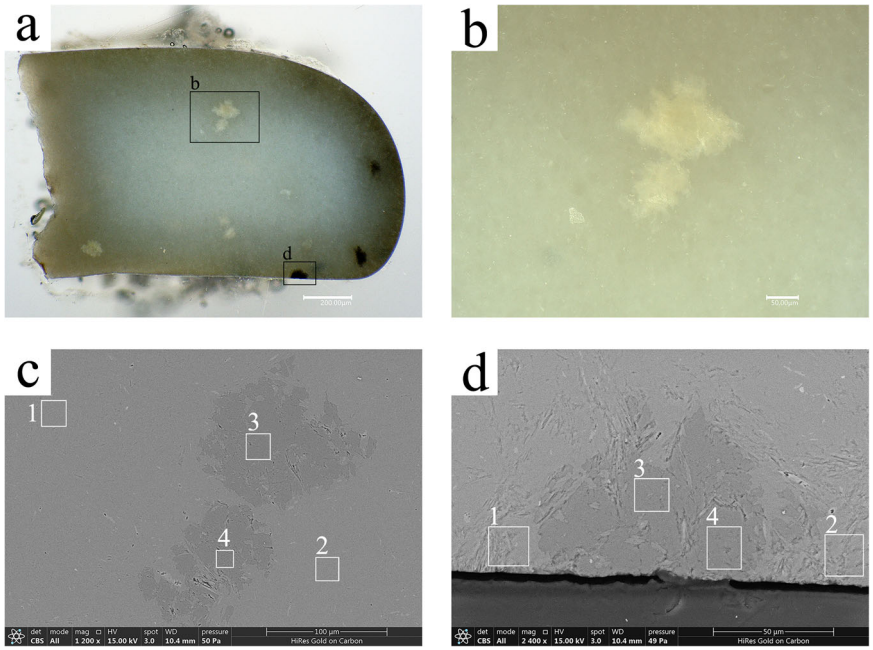

Fig. 2 | Sample image of K7QW-Y-32 (**a**, **b** ultra-depth-of-field microscopic image; **c** BSE image of the matrix and yellowish inclusions area; and **d** BSE image of the brownish-black inclusions area).

conservation. This study selected several typical tremolite jade artifacts and attempted to identify their deterioration mechanisms by examining morphology, compositional analysis, and phase analysis.

Methods

Samples

After a systematic observation of the excavated jades, three representative samples were selected (Fig. 1). Samples K7QW-Y-32 and K7QW-Y-112 were chosen from pit K7, and sample K3QW-557 was chosen from pit K3. Sample K7QW-Y-32 is a fragment of a *yuan* (瑗), with only three segments remaining. After cleaning, it exhibits a pale yellow coloration with a waxy luster, and its texture is compact and dense. K7QW-Y-112 is a fragment of a *zhang* (璋), showing a gray-brown coloration with slight surface powdering. K3QW-557 exhibits severe powdering and whitening, and its original shape is unrecognizable.

Analytical techniques

The samples studied in this paper were small fragments of jade. These samples were inlaid with epoxy resin, sanded, and polished before analysis.

Ultra-depth-of-field microscope. The profile shape of the jade samples was observed using an ultra-depth-of-field microscope (KEYENCE Digital Microscope VHX-7000). Equipped with a 3.19-million-pixel CMOS image sensor, it utilizes a high-resolution HR lens that combines a large depth of field with high resolution, offering magnification from 20× to 2000×.

Scanning electron microscope–X-ray energy dispersive spectrometer (SEM–EDS). A scanning electron microscope (Thermo Scientific, Quattro S) equipped with an X-ray energy dispersive spectrometer (Bruker QUANTAX EDS) was used to characterize the microscopic morphology and elemental composition of the jade samples. The analyses were conducted in a low-vacuum environment using backscattered electron imaging, with an operating voltage of 15 kV, a working distance of 10 mm, and a sampling time of 60 s. The oxide data were normalized to one decimal place.

Laser microscopic confocal Raman spectrometer (Raman). The material composition of the jade samples was characterized using a laser microscopic confocal Raman spectrometer (RENISHAW inVia), which was equipped with a research-grade Leica microscope offering a spatial resolution of less than 0.5 μm. The experimental conditions were as follows: an excitation wavelength of 785 nm, a scanning time of 10 s, and 30 scans.

Fourier transform infrared spectroscopy (FTIR). FTIR (Thermo Fisher Scientific) was used to analyze the phase transitions of the samples. The system was equipped with a micro-infrared mainframe (Nicolet iN10), an attenuated total reflection (ATR) accessory, and a transmission accessory (Nicolet iS10/iZ10 auxiliary optics platform). For sample preparation, the jade and potassium bromide were mixed in an agate mortar at a ratio of 1:150–200. After thorough grinding and mixing, the resulting mixture was pressed into transparent circular

slices with a thickness of 0.1–1.0 mm for testing in the sample chamber. The experimental conditions were as follows: the detector was a DTGS KBr with a scanning range of 4000–400 cm^{-1} and a resolution of 4 cm^{-1}, using 32 background scans and 32 sample scans.

Results

SEM–EDS and Raman spectral analyses

The SEM image of sample K7QW-Y-32 is shown in Fig. 2, and the EDS results are in Table 1. The sample was well-preserved, and the jade matrix appeared greenish with fractured areas. The major elements in the jade matrix (Fig. 2c, EDS1 and EDS2) were close to the theoretical values for tremolite. Raman spectra confirmed that the sample was tremolite (Fig. 5a)[13,14].

Table 1 | Results of EDS analyses of sample K7QW-Y-32 (wt/%)

Test area		Na_2O	MgO	Al_2O_3	SiO_2	K_2O	CaO	FeO	Presumably phase
c	1	0.2	25.7	0.2	60.6	–	12.9	0.4	Tremolite
	2	0.2	25.6	0.8	61.4	–	11.8	0.4	Tremolite
	3	8.2	6.9	13.9	67.4	–	3.6	–	Albite
	4	7.2	9.2	12.3	66.3	–	5.0	–	Albite
d	1	0.2	25.5	0.8	61.2	–	11.9	0.4	Tremolite
	2	0.4	25.2	0.8	61.4	–	12.0	0.2	Tremolite
	3	7.9	6.4	14.1	67.7	0.2	3.6	–	Albite
	4	8.8	6.1	14.6	67.7	–	2.8	–	Albite

The elemental composition of the yellow-greenish area at the edge of the sample was similar to that of the greenish matrix. The main elements of the yellowish inclusions (Fig. 2c, EDS3 and EDS4) and brownish-black inclusions (Fig. 2d, EDS3 and EDS4) were Si, Al, and Na, which were preliminarily presumed to be albite ($NaAlSi_3O_8$), as identified by the Raman spectra shown in Fig. 5b.

The SEM image of sample K7QW-Y-112 is shown in Fig. 3, and the EDS results are in Table 2. The sample was brownish-yellow overall, with some areas showing signs of whitening. The whitened areas were porous, and acicular crystals were exposed within the holes. Brown attachments were found locally on the outermost part of the surface, corresponding to the dark grey areas in the SEM BSE images (Fig. 3d, EDS1 and EDS2). These attachments were primarily clay minerals from the soil, containing elements such as Si, Al, Fe, Mg, Ca, and K. Beneath the attachments lay the jade matrix (Fig. 3d, EDS3 and EDS4), as confirmed by both EDS and Raman spectroscopy (Fig. 5c).

The composition of a few acicular crystals within the holes (Fig. 3e, EDS1) was similar to that of the dense area. The Ca content in most of the acicular crystals (Fig. 3e, EDS2, EDS3, and EDS4) was significantly elevated, while the Mg content was noticeably reduced. Raman spectra (Fig. 5c) indicated that their main physical phase remained tremolite.

The regions shown in Fig. 3f, EDS3 and EDS4 correspond to the materials enveloping the acicular crystals within the corrosion holes. Their elemental compositions were similar to those observed in the outermost thin layer, though with marginally elevated Mg and Ca contents. The Raman spectra (Fig. 5d) of the acicular crystals (Fig. 3e, EDS2), the brown

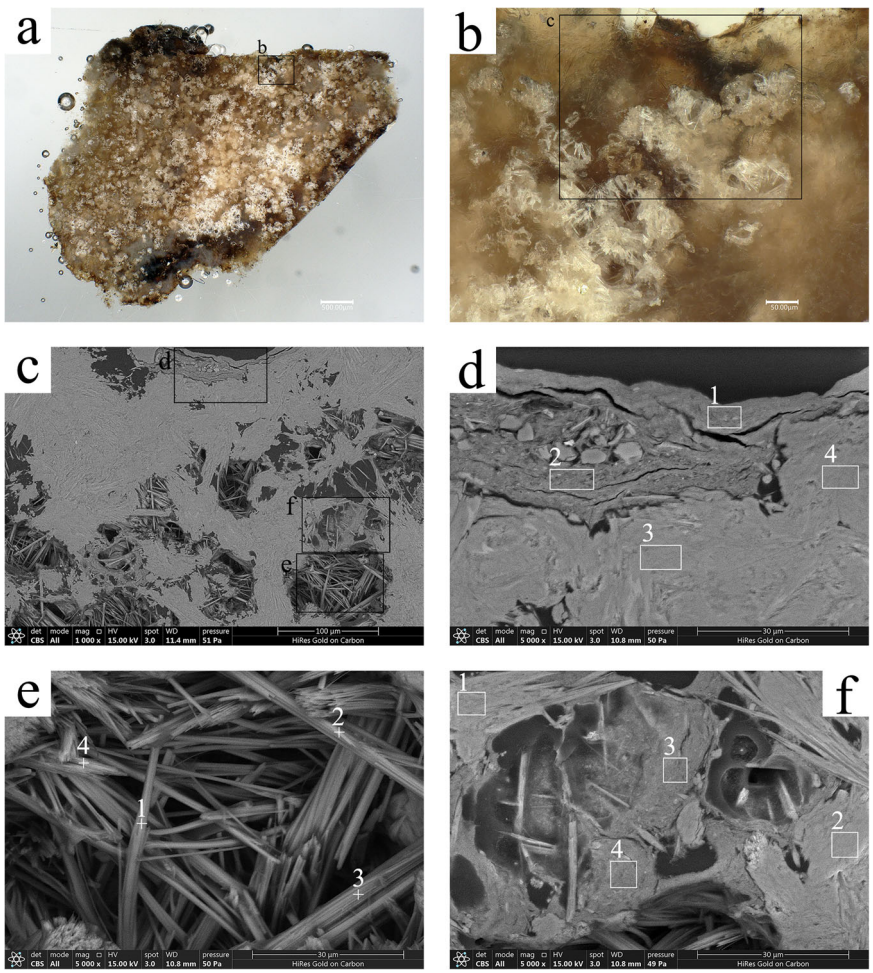

Fig. 3 | Sample image of K7QW-Y-112 (**a**, **b** ultra-depth-of-field microscopic image; **c** BSE image of the area of Fig. 3b; **d** BSE image of the brown attachments; **e** BSE image of the acicular crystals; and **f** BSE image of the materials wrapped outside the acicular crystals).

Table 2 | Results of EDS analyses of sample K7QW-Y-112 (wt/%)

Test area		Na_2O	MgO	Al_2O_3	SiO_2	P_2O_5	Cl	K_2O	CaO	TiO_2	FeO	Cu_2O	Presumably phase
d	1	0.6	5.8	23.4	55.7	0.7	0.2	2.3	2.6	0.8	7.3	0.7	Soil components
	2	0.6	6.2	21.2	57.9	0.4	0.2	2.6	3.0	0.7	6.2	1.0	
	3	0.5	26.2	0.9	60.4	–	0.1	0.2	11.5	–	0.4	–	Tremolite
	4	0.5	25.6	1.0	60.2	–	–	–	12.1	–	0.7	–	Tremolite
e	1	0.1	26.6	1.4	59.9	–	–	–	11.2	–	0.8	–	Tremolite
	2	0.0	22.4	0.3	62.5	–	0.1	–	14.2	–	0.5	–	Pyroxene trends
	3	0.1	21.3	0.8	62.2	–	0.2	–	15.3	–	0.0	–	Pyroxene trends
	4	0.2	21.3	0.4	63.5	–	–	–	14.4	–	0.2	–	Pyroxene trends
f	1	0.4	26.1	0.8	60.1	–	0.1	–	12.1	–	0.4	–	Tremolite
	2	0.4	26.4	0.2	61.1	–	–	–	11.6	–	0.3	–	Tremolite
	3	0.3	10.7	18.7	55.7	0.4	0.2	2.2	4.3	0.3	6.5	0.7	Soil components
	4	0.4	10.8	19.6	56.2	0.1	0.2	2.1	4.7	0.5	4.9	0.5	

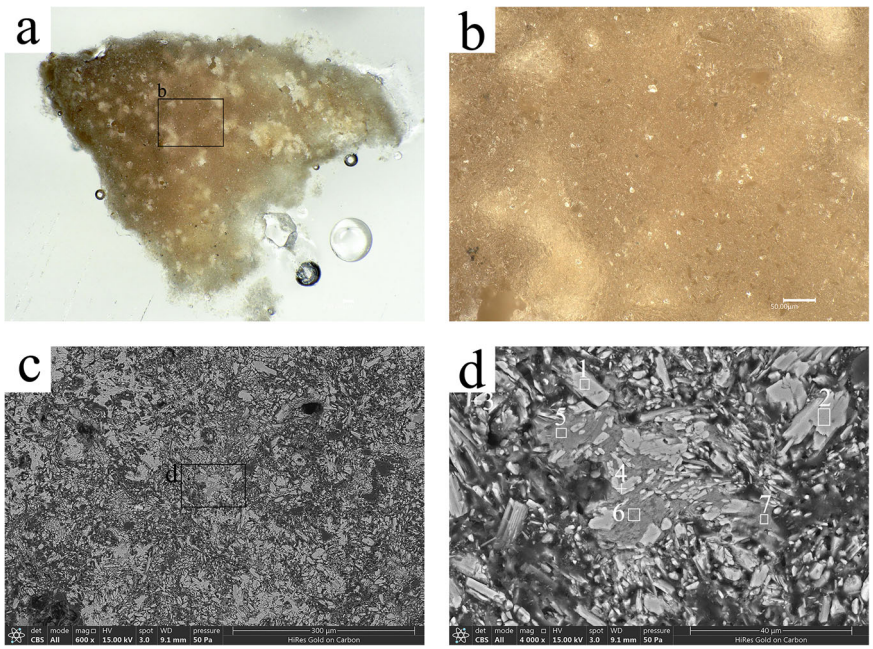

Fig. 4 | Sample image of K3QW-557 (**a**, **b** ultra-depth-of-field microscopic image; **c** BSE image of the area of Fig. 4b; and **d** partially enlarged BSE image in Fig. 4c).

Table 3 | Results of EDS analyses of sample K3QW-557 (wt/%)

Test area		MgO	Al_2O_3	SiO_2	P_2O_5	SO_3	Cl	K_2O	CaO	TiO_2	FeO	Cu_2O	Presumably phase
d	1	16.3	1.9	56.0	–	–	0.1	–	25.3	–	0.4	–	Diopside
	2	16.3	1.4	56.1	–	–	–	–	26.0	–	0.2	–	Diopside
	3	16.4	1.3	55.4	–	–	0.2	–	26.1	–	0.6	–	Diopside
	4	16.2	2.1	53.6	–	–	–	–	27.8	–	0.3	–	Diopside
	5	33.3	17.4	42.8	–	–	–	–	5.3	–	1.3	–	Enstatite
	6	34.7	18.5	41.5	–	–	–	–	4.8	–	0.6	–	Enstatite
	7	10.6	16.2	54.1	0.2	0.5	0.4	1.4	9.5	0.4	6.5	0.3	Soil components

attachments (Fig. 3d, EDS1), and the materials within the holes (Fig. 3f, EDS3) in the range of 0–3200 cm^{-1} all exhibit a characteristic strong hump-shaped fluorescence background.

The SEM image of sample K3QW-557 is shown in Fig. 4, and the EDS results are in Table 3. The sample was pale yellow and opaque, and it had completely powdered and whitened. This type of sample exhibited a loose structure, which allowed the epoxy resin to seep through during embedding. The BSE image showed that the broken crystals consisted of irregular, small, lumpy, granular light grey crystals, as well as some dark grey materials. The components of the light grey crystals (Fig. 4d, EDS1, EDS2, EDS3, and EDS4) were similar to diopside ($CaMgSi_2O_6$), with the theoretical components as follows: CaO: 25.9%, MgO: 18.5%, SiO_2: 55.6%. Raman spectra (Fig. 5e) confirmed that the jade phase was predominantly diopside[15,16]. In the area in Fig. 4d, EDS2 detected the presence of both

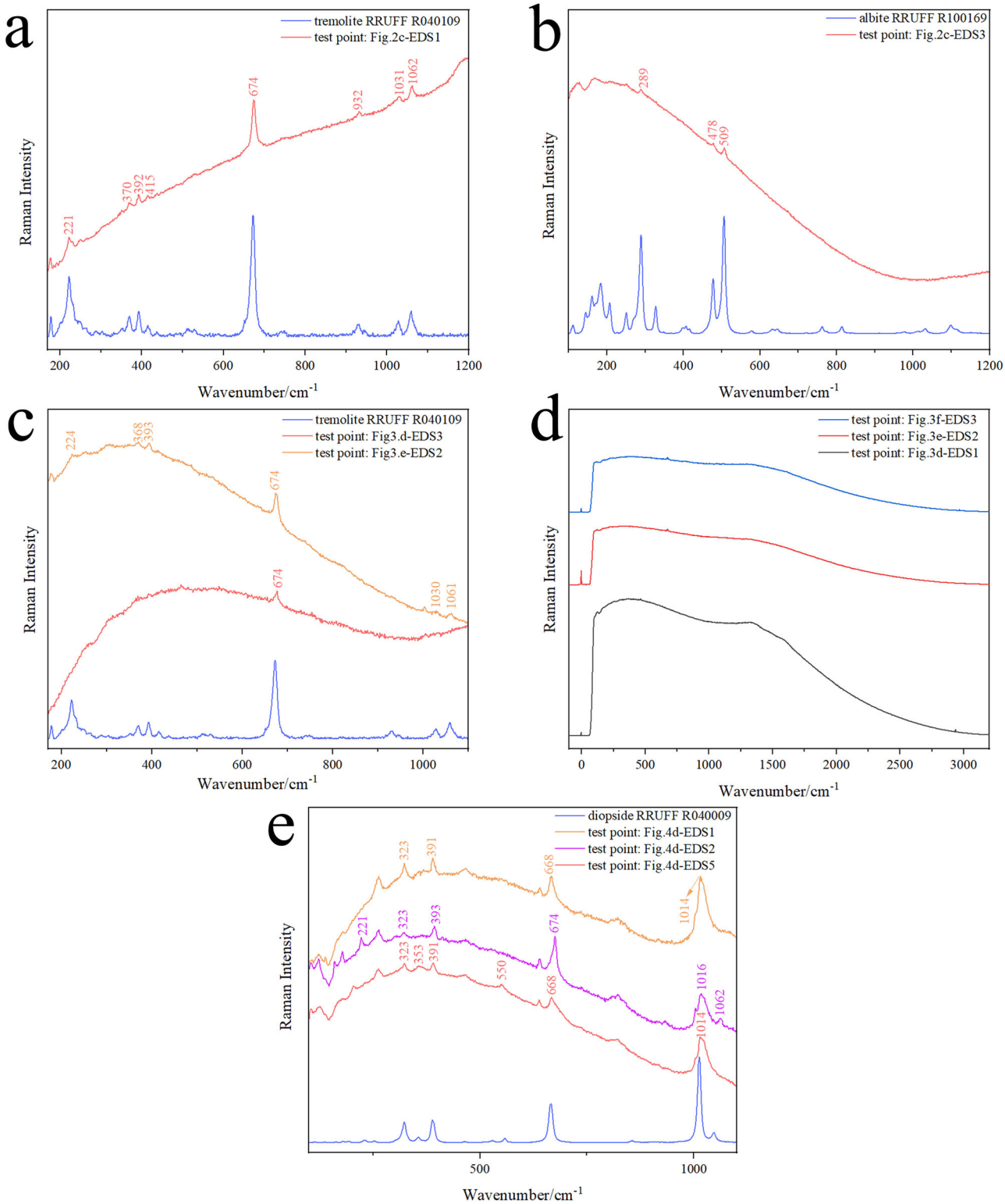

Fig. 5 | Raman spectral image (**a** sample K7QW-Y-32 matrix—tremolite; **b** Sample K7QW-Y-32 inclusions—albite; **c** sample K7QW-Y-112 material—tremolite; **d** sample K7QW-Y-112 fluorescent background—hump-shaped curves; and **e** sample K3QW-557 material—diopside).

tremolite and diopside by Raman spectroscopy. The dark grey areas (Fig. 4d, EDS5 and EDS6) were amorphous and predominantly contained Si and Mg elements, with elemental ratios resembling those of enstatite ($Mg_2Si_2O_6$). The Raman spectra of these areas (Fig. 5e) closely matched the pyroxene $Di_{40}En_{60}$[17].

Infrared spectral analyses

An appropriate amount of powder from samples K7QW-Y-32 and K3QW-557 was scraped and subjected to rigorous testing by using the IR-KBr method. The results are shown in Fig. 6. The infrared spectra indicated that sample K7QW-Y-32 was identified as tremolite[18,19].

For sample K3QW-557, the bands at 1073 cm^{-1}, 953 cm^{-1}, 920 cm^{-1}, 860 cm^{-1}, 672 cm^{-1}, and 635 cm^{-1} exhibited characteristics of diopside, which were associated with Si–O vibrations[20]. The infrared spectroscopy results are consistent with those obtained from Raman spectroscopy and can corroborate each other.

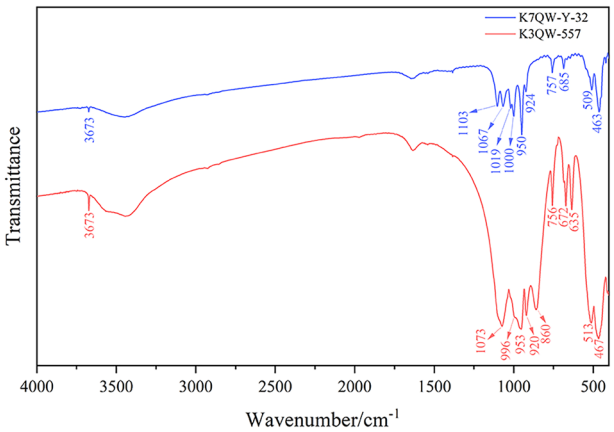

Fig. 6 | Infrared spectra of K7QW-Y-32 and K3QW-557.

Discussion

The preservation states of jade artifacts unearthed from different positions in the K3–K8 sacrificial pits at the Sanxingdui site exhibited considerable differences. The three representative samples discussed in this paper showed distinct deterioration features. The jade artifact K7QW-Y-32, which had not been subjected to heat, remained in relatively good condition. It is still dense, with no significant deterioration observed in the jade matrix. The phase of sample K7QW-Y-112 is still identified as tremolite, but its structure is loose, with numerous internal holes. The acicular crystals exposed within these holes showed a tendency to transform into pyroxene. Additionally, attachments with soil components were present both on the surface and inside the holes of the sample. Sample K3QW-557 had almost completely decomposed into pyroxene (diopside and enstatite), dominated by diopside. The artifact was severely whitened and powdered, with a highly fragmented internal structure and significantly reduced mechanical strength. The jade artifacts unearthed from the K3–K8 sacrificial pits at the Sanxingdui site were burned before being buried[5]. The deterioration was influenced by the placement of the artifacts and their distance from the heat source.

The pyroxene formed by the heating of tremolite was characterized by fragmented crystals with low crystallinity, making it more prone to destruction[21]. Pyroxene jade was more susceptible to dissolution and

Fig. 7 | Schematic deterioration of jade artifacts from the Sanxingdui sacrificial pits - profiles.

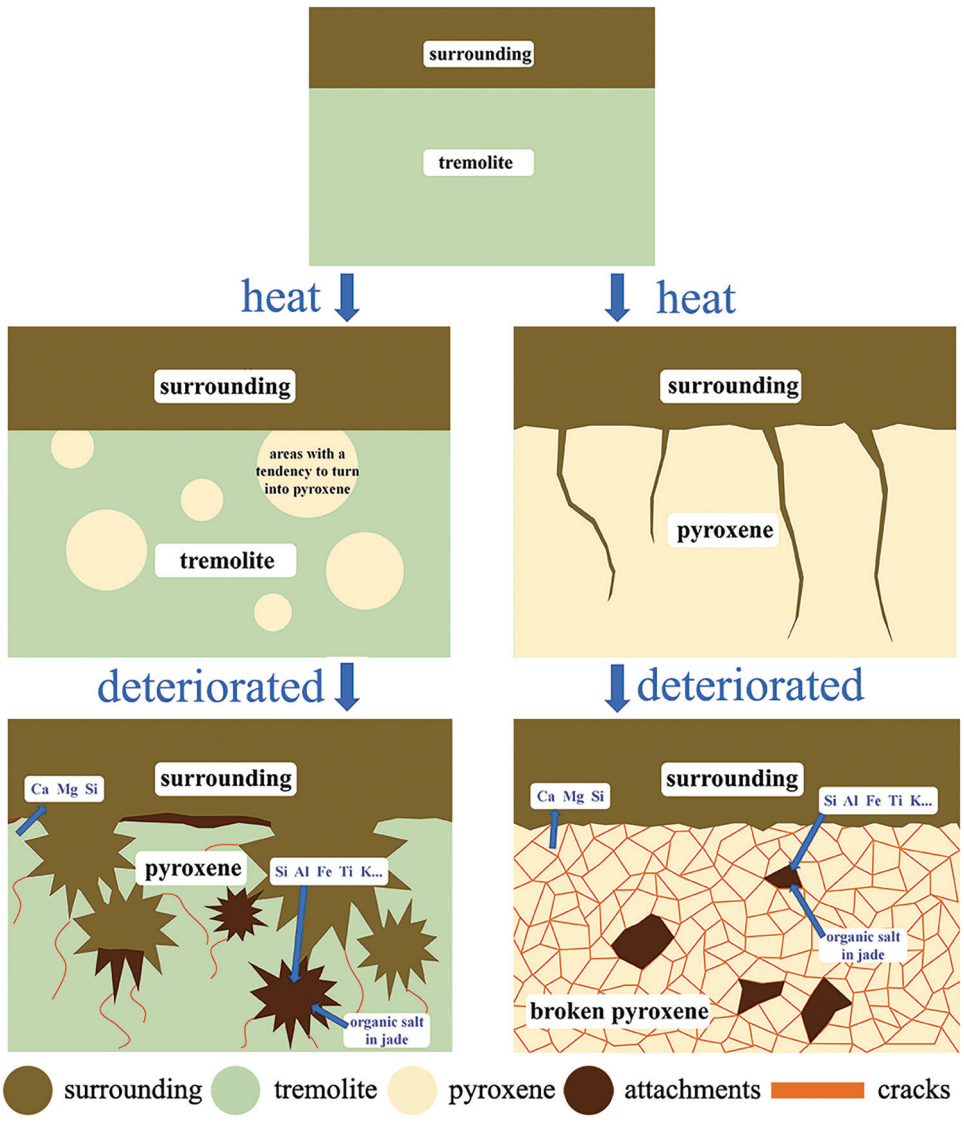

leaching in the burial environment, leading to the loss of elements such as Ca, Mg, and Si. This gave rise to the fracture of crystals within the jade artifacts, leading to a loose structure with numerous cracks and holes. Soluble components in the soil, carried by water, infiltrated the jade, accelerating its further weathering. The deterioration process of tremolite jade is shown in Fig. 7.

In conclusion, this study reveals that the deterioration of jade artifacts unearthed from the sacrificial pits at the Sanxingdui site is related to the sacrificial activities prior to their burial. Heating exposure at high temperatures can lead to the thermal decomposition of tremolite into a pyroxene group dominated by diopside. Through comprehensive analyses of the jade artifacts' structural composition and mineral phases, this study elucidates that tremolite jade artifacts within the sacrificial pits have transformed to varying degrees of pyroxene. Some tremolite artifacts retain their original structure, while others have locally transformed into pyroxene, and some have completely transformed into pyroxene.

Compared to tremolite jade artifacts, pyroxene jade artifacts were more prone to environmental influences, resulting in more severe deterioration. Attachments containing external soil components can be observed on the surfaces of artifacts with localized pyroxenization, as well as within its deterioration holes. Jade artifacts with complete pyroxenization show the highest degree of deterioration, characterized by severe whitening and powdering. Both jade artifacts with localized pyroxenization and those with complete pyroxenization should be reinforced by using highly permeable materials to prevent further powdering and deterioration in practice.

Data availability

No datasets were generated or analysed during the current study.

Received: 6 July 2024; Accepted: 14 April 2025;
Published online: 05 May 2025

References

1. Archaeological Team at the Sanxingdui Site Sacrificial Area. Sacrificial area of the Sanxingdui Site in Guanghan City, Sichuan (in Chinese). *Archaeology*. **7**, 15–33+2 (2022).
2. Li, Y., Qiu, T., Guo, J. & Li, Y. New discoveries at the Sanxingdui Bronze Age site in south-west China. *Antiquity* **97**, e4 (2023).
3. Sichuan Provincial Cultural Relics and Archeology Research Institute, National Center for Archaeology. Joint Laboratory for Archaeological Chronology, School of Archaeology and Museology, Peking University. AMS Radiocarbon dating of K4 sacrificial pit at Sanxingdui Site in Guanghan City, Sichuan (in Chinese). *Sichuan Cult. Relics* **2**, 117–120 (2021).
4. Sichuan Provincial Institute of Cultural Relics and Archeology. *Excavation of the Sacrificial Pits at Sanxingdui* (in Chinese) (Cultural Relics Press, Beijing, 1999).
5. Lu, H. et al. Characterizing ancient jade by on-site analysis in Sanxingdui, China. *Herit. Sci.* **11**, 121 (2023).
6. Guo, Y. et al. The sacrificial record in burial pits of the late Shang Dynasty: evidences from the chroma and magnetic properties of the Sanxingdui site, Sichuan, China. *Herit. Sci.* **11**, 258 (2023).
7. Wang, R., Mai, Y. & Lin, L. Burnt jade sacrifices in the Chinese Neolithic: the Liangzhu cemetery at Sidun. *Antiquity* **96**, 1495–1514 (2022).
8. Wang, R., Wang, C. & Tang, J. A jade parrot from the tomb of Fu Hao at Yinxu and Liao sacrifices of the Shang Dynasty. *Antiquity* **92**, 368–382 (2018).
9. Wang, R. Progress review of the scientific study of Chinese ancient jade. *Archaeometry* **53**, 674–692 (2011).
10. Wang, Y. et al. Analysis of whitening mechanism of ancient tremolite jade: taking some of the jades excavated from the Sanxingdui site as examples (in Chinese). *Sci. Conserv. Archaeol.* **36**, 17–33 (2024).
11. Lu, H. et al. A test report on the formulae of the jade and stone objects unearthed at the Sanxingdui ruin site and other related issues (in Chinese). *J. Palace Mus.* **64**, 123–142+147 (2021).
12. Liu, J., Ming, W., Wang, Y., Wang, J. & Yu, J. Traceability study of large jade materials unearthed at the Sanxingdui site (in Chinese). *Sichuan Cult. Relics* **38**, 84–94 (2021).
13. Rinaudo, C., Belluso, E. & Gastaldi, D. Assessment of the use of Raman spectroscopy for the determination of amphibole asbestos. *Miner. Mag.* **68**, 455–465 (2004).
14. Wang, R. & Zhang, W. Application of Raman spectroscopy in the nondestructive analyses of ancient Chinese jades. *J. Raman Spectrosc.* **42**, 1324–1329 (2011).
15. Chen, T. A Raman spectroscopic study of heat-treated nephrite. *Phase Transit.* **81**, 205–216 (2008).
16. Wang, R. & Zhang, B. Raman spectra of pyroxene (in Chinese). *Spectrosc. Spect. Anal.* **30**, 376–381 (2010).
17. Tribaudino, M., Mantovani, L., Bersani, D. & Lottici, P. Raman spectroscopy of (Ca, Mg) $MgSi_2O_6$ clinopyroxenes. *Am. Miner.* **97**, 1339–1347 (2012).
18. Wang, D., Xu, Z., Sun, M. & Cao, S. Study on the IR spectrum of jasper of different origin (in Chinese). *Infrared Tech.* **31**, 698–701+707 (2009).
19. Korybska-Sadło, I., Gil, G., Gunia, P., Horszowski, M. & Sitarz, M. Raman and FTIR spectra of nephrites from the Złoty Stok and Jordanów Śląski (the Sudetes and Fore-Sudetic Block, SW Poland). *J. Mol. Struct.* **1166**, 40–47 (2018).
20. Omori, K. Analysis of the infrared absorption spectrum of diopside. *Am Miner* **56**, 1607–1616 (1971).
21. Bao, Y., Zhao, C., Li, Y. & Yun, X. A method of determining heated ancient nephrite jades in China. *Sci. Rep.* **8**, 13523 (2018).

Acknowledgements

We want to thank Fei Tang, the general director of the Sichuan Provincial Institute of Cultural Relics and Archaeology, and Zhenbin Xie, the deputy director of the Sichuan Provincial Institute of Cultural Relics and Archaeology, as well as Professor Cong Deng, Yishu Wang, Shasha Long, Yu Wang, Ziyu Xu, and other students from Shandong University for their help. We are thankful for the support of the Sichuan Science and Technology Program: Conservation and Research of Jade Artifacts Unearthed at the Sanxingdui Site (2024YFFK0125), and the 2023 Young Cultural and Museum Talents Cultivation Program in Shandong Province: Ancient Jade Physical Composition and Classification.

Author contributions

Q.M. provided support and guidance for this study. J.L. and H.R. provided study samples. C.X. completed all analytical tests, interpreted the data, and wrote the manuscript. Y.W. guided and revised the manuscript. H.W. and H.F. provided advice. All authors read and approved the final manuscript.

Competing interests

The authors declare no competing interests.

Additional information

Correspondence and requests for materials should be addressed to Yunpeng Wang or Qinglin Ma.